A Biphasic, Anisotropic Model of the Aortic Wall

Mark Johnson
Northwestern University,
Evanston, IL

John M. Tarbell
Pennsylvania State University,
University Park, PA 16802

A biphasic, anisotropic elastic model of the aortic wall is developed and compared to literature values of experimental measurements of vessel wall radii, thickness, and hydraulic conductivity as a function of intraluminal pressure. The model gives good predictions using a constant wall modulus for pressures less than 60 mmHg, but requires a strain-dependent modulus for pressures greater than this. In both bovine and rabbit aorta, the tangential modulus is found to be approximately 20 times greater than the radial modulus. These moduli lead to predictions that, when perfused in a cylindrical geometry, the aortic volume and its specific hydraulic conductivity are relatively independent of perfusion pressure, in agreement with experimental measurements. M, the parameter that relates specific hydraulic conductivity to tissue dilation, is found to be a positive quantity correcting a previous error in the literature. [DOI: 10.1115/1.1339817]

Keywords: Elasticity, Hydraulic Conductivity, Bovine, Rabbit

Introduction

A number of studies have examined fluid and macromolecular transport across the wall of the aorta (e.g., [1–8]). As the aortic wall is an elastic structure that undergoes significant changes in dimension with changes in intraluminal pressure, a complete characterization of transport across this wall must necessarily include a structural analysis. Early studies of the structure modeled the aorta as an isotropic, single-phase material [9]. However, it has been recognized that the aorta is both anisotropic [10–12] and biphasic [13,5,8].

Klanchar and Tarbell [5] and Kim and Tarbell [7] modeled the aortic wall as a biphasic material and were able to find closed-form expressions to characterize both the elastic response and the transport characteristics of the aortic wall. Whale et al. [14] modeled the aortic wall as an anisotropic, single-phase material and also found closed-form expressions that characterized the elastic response of such a vessel.

In this paper, we combine these two models to yield a biphasic, anisotropic model of the aortic wall that still allows for a closed-form solution. We show that the new model agrees well with experimental data at low perfusion pressures (less than 100 mmHg), and when we include nonlinearity of the elastic moduli, the model shows good agreement with data taken over a wide range of perfusion pressures.

Biphasic, Anisotropic Model of the Aortic Wall

We model the aortic wall as an axially confined, hollow cylinder (inside radius a, outside radius b). A force balance, relating the stresses (σ) on a differential cylindrical element, yields [12]:

$$\frac{d\sigma_r}{dr}+\left(\frac{\sigma_r-\sigma_t}{r}\right)=0 \tag{1}$$

where r is the radial direction, and t is the tangential direction. These stresses can be related to the effective stresses defined as $S=\sigma+P$, where P is the hydrostatic pressure. Thus, we find that [5]:

$$\frac{dS_r}{dr}+\left(\frac{S_r-S_t}{r}\right)=\frac{dP}{dr} \tag{2}$$

The strains in this medium are related to the radial displacements (u) of the cylinder as:

$$\varepsilon_r=\frac{du}{dr};\quad \varepsilon_t=\frac{u}{r} \tag{3}$$

To relate these strains to the stresses, we assume the vessel wall to be a linear, transversely isotropic material with an anisotropic axis in the radial direction [11,15,12]. As the material is modeled as biphasic, the strains are related to the effective stresses [5] rather than the total stress. The generalized Hooke's law for a transversely isotropic material are given by Lehknitskii [16] as:

$$\varepsilon_r=\frac{1}{E'}S_r-\frac{\nu'}{E'}S_t-\frac{\nu'}{E'}S_z \tag{4a}$$

$$\varepsilon_t=-\frac{\nu'}{E'}S_r+\frac{1}{E}S_t-\frac{\nu}{E}S_z \tag{4b}$$

$$\varepsilon_z=-\frac{\nu'}{E'}S_r-\frac{\nu}{E}S_t+\frac{1}{E}S_z \tag{4c}$$

where E is Young's modulus in the plane of isotropy, E' is Young's modulus in the direction perpendicular to the plane of isotropy, ν is Poisson's ratio characterizing contraction or expansion in the plane of isotropy in the presence of tension or compression in that same plane, and ν' is Poisson's ratio in the direction perpendicular to the plane of isotropy. The plane of isotropy is the cylindrical surface defined by the axial (z) and tangential (t) directions. Note that since effective stresses are used in the constitutive relationships (thus implicitly assuming that the solid phase is intrinsically incompressible), a uniform hydrostatic change in pressure on the medium will not generate strains.

For a thick-walled vessel with axially constrained ends, the deformation is one of plane strain ($\varepsilon_z=0$), which yields from Eq. 4(c):

$$S_z=\frac{E\nu'}{E'}S_r+\nu S_t \tag{5}$$

Equations 4(a) and 4(b) then lead to:

$$S_r=\frac{\beta_{22}\varepsilon_r-\beta_{12}\varepsilon_t}{\beta_{11}\beta_{22}-\beta_{12}^2} \tag{6}$$

and

Contributed by the Bioengineering Division for publication in the JOURNAL OF BIOMECHANICAL ENGINEERING. Manuscript received by the Bioengineering Division July 2, 1999; revised manuscript received August 29, 2000. Associate Editor: J. B. Grotberg.

$$S_t = \frac{-\beta_{12}\varepsilon_r + \beta_{11}\varepsilon_t}{\beta_{11}\beta_{22} - \beta_{12}^2} \tag{7}$$

where the constants are defined as:

$$\beta_{11} = \frac{1}{E'}\left(1 - \nu'^2 \frac{E}{E'}\right), \quad \beta_{22} = \frac{1}{E}(1-\nu^2), \quad \beta_{12} = \frac{-\nu'}{E'}(1+\nu) \tag{8}$$

Introducing Eqs. (6) and (7) into Eqs. (2) and (3), we find that

$$\frac{d^2u}{dr^2} + \frac{1}{r}\frac{du}{dr} - \frac{\beta_{11}}{\beta_{22}}\frac{u}{r^2} = \frac{\beta_{11}\beta_{22} - \beta_{12}^2}{\beta_{22}}\frac{dP}{dr} \tag{9}$$

The pressure gradient is determined by Darcy's law:

$$\frac{dP}{dr} = -\frac{\mu Q}{2\pi r L K} \tag{10}$$

where μ is the fluid viscosity, Q is the flowrate passing across the aortic wall, L is the length of the vessel and K is its specific hydraulic conductivity [17,12]. The specific hydraulic conductivity is assumed to depend on the bulk dilation (Ψ) of the medium. Lai and Mow [18] proposed an exponential form, $K = K_0 \exp(M\Psi)$, which was linearized by Klanchar and Tarbell [5] as:

$$\frac{1}{K} = \frac{1 - M\Psi}{K_0} \tag{11}$$

where M and K_0 are material properties. This approximation is reasonable for $M\Psi << 2$, a condition that we will see is met for aorta when perfused in a cylindrical geometry, but not when a piece of aortic wall is perfused in a flat geometry, as addressed in the appendix.

We note here that M is a positive constant since the specific hydraulic conductivity of a medium decreases when it is compressed. Klanchar and Tarbell [5] allowed M to be negative, a point we address further in the discussion section.

Since the bulk dilation can be related to the strain field as $\Psi = du/dr + u/r$, substitution of Eq. (11) into Eq. (10) yields:

$$\frac{dP}{dr} = -\frac{\mu Q}{2\pi L K_0}\left(\frac{1}{r} - \frac{M}{r}\frac{du}{dr} - \frac{Mu}{r^2}\right) \tag{12}$$

Substituting this result into Eq. (9) yields:

$$\frac{d^2u}{dr^2} + \frac{1 - M\alpha}{r}\frac{du}{dr} - \left(\frac{\beta_{11}}{\beta_{22}} + M\alpha\right)\frac{u}{r^2} = -\frac{\alpha}{r} \tag{13}$$

where

$$\alpha \equiv \frac{\mu Q}{2\pi L K_0}\left[\frac{\beta_{11}\beta_{22} - \beta_{12}^2}{\beta_{22}}\right] \tag{14}$$

The general solution to this differential equation is:

$$u(r) = A_1 r^{k_1} + A_2 r^{k_2} + \frac{\alpha r}{2M\alpha + \left(\frac{\beta_{11}}{\beta_{22}} - 1\right)} \tag{15}$$

where A_1 and A_2 are constants of integration and

$$\frac{d^2u}{dr^2} + \frac{1 - M\alpha}{r}\frac{du}{dr} - \left(\frac{\beta_{11}}{\beta_{22}} + M\alpha\right)\frac{u}{r^2} = -\frac{\alpha}{r} \tag{16}$$

If $\beta_{11} = \beta_{22}$, Eq. (16) reduces to the same form found by Klanchar and Tarbell [5] and if $M = 0$, then the result found by Whale et al. [14] is recovered.

For an unrestricted artery, we now apply the condition of zero effective radial stress at the boundaries,

$$S_r(r=a) = S_r(r=b) = 0 \tag{17}$$

Using Eqs. (6), the condition of zero effective radial stress is shown to be equivalent to the following condition:

$$\beta_{22}\varepsilon_r = \beta_{12}\varepsilon_t \tag{18}$$

Applying this condition at the boundaries ($r=a$ and $r=b$), Eq. (15) becomes:

$$\frac{u(r)}{r} = \alpha^*\left\{\frac{(\beta_{12} - \beta_{22})}{\gamma^{k_2-1} - \gamma^{k_1-1}}\left[\frac{(\gamma^{k_2-1} - 1)(r/a)^{k_1-1}}{\beta_{22}k_1 - \beta_{12}} - \frac{(\gamma^{k_1-1} - 1)(r/a)^{k_2-1}}{\beta_{22}k_2 - \beta_{12}}\right] + 1\right\} \tag{19}$$

where $\gamma \equiv b/a$ and

$$\alpha^* \equiv \frac{\alpha}{2M\alpha + \left(\frac{\beta_{11}}{\beta_{22}} - 1\right)} \tag{20}$$

In particular, evaluating Eq. (19) at the boundaries, we find that:

$$\frac{b - b_0}{b} = \alpha^*\left\{\frac{(\beta_{12} - \beta_{22})}{\gamma^{k_2-1} - \gamma^{k_1-1}}\left[\frac{(\gamma^{k_2-1} - 1)\gamma^{k_1-1}}{\beta_{22}k_1 - \beta_{12}} - \frac{(\gamma^{k_1-1} - 1)\gamma^{k_2-1}}{\beta_{22}k_2 - \beta_{12}}\right] + 1\right\} \tag{21}$$

and

$$\frac{a - a_0}{a} = \alpha^*\left\{\frac{(\beta_{12} - \beta_{22})}{\gamma^{k_2-1} - \gamma^{k_1-1}}\left[\frac{(\gamma^{k_2-1} - 1)}{\beta_{22}k_1 - \beta_{12}} - \frac{(\gamma^{k_1-1} - 1)}{\beta_{22}k_2 - \beta_{12}}\right] + 1\right\} \tag{22}$$

where a_0 and b_0 are the inner and outer radius of the vessel when $Q = 0$.

To find the pressure drop (ΔP) across the aortic wall for a given flowrate, we integrate Eq. (12) across the aortic wall to find that:

$$\Delta P = \frac{\mu Q}{2\pi L K_0}\left\{(1 - 2M\alpha^*)\ln\gamma - M\alpha^*\frac{(\beta_{11} + \beta_{22} + 2\beta_{12})(\beta_{22} - \beta_{12})(k_2 - k_1)(\gamma^{k_1-1} - 1)(\gamma^{k_2-1} - 1)}{(\beta_{22}k_1 - \beta_{12})(\beta_{22}k_2 - \beta_{12})(k_1 - 1)(k_2 - 1)(\gamma^{k_2-1} - \gamma^{k_1-1})}\right\} \tag{23}$$

Finally, it is useful to consider the thin wall limit of Eqs. (21)–(23). Letting $\delta = b - a << a$, we find that in this limit:

$$\frac{b - b_0}{b} = \beta_{22}\left(\frac{\Delta P b}{\delta}\right), \tag{24}$$

$$\frac{\delta - \delta_0}{\delta} = \beta_{12}\left(\frac{\Delta P b}{\delta}\right) \tag{25}$$

and

$$\Delta P = \frac{\frac{\mu Q}{2\pi L K_0}\left(\frac{\delta}{a}\right)}{\left[1 + \frac{\mu Q(\beta_{12} + \beta_{22})M}{2\pi L K}\right]} \tag{26}$$

Equations (24) and (25) can be used in combination with experi-

mental data to estimate tissue moduli. For low flowrates, Eq. (26) reduces to the familiar form used to estimate specific hydraulic conductivity.

Application of the Model to the Data of Whale et al.

Whale et al. [14] used a anisotropic, single-phase model to describe the deformation of the bovine aorta. We use their data to generate parameter values for our new extended model and then compare their model predictions to those of the new model.

The parameter values required are E, E', ν, ν', and M. For the elastic parameters, we use the same best-fit parameters as Whale et al. ($E=460$ kPa, $E=20$ kPa, $\nu=0.3$) with the exception of ν', which we allow to vary in the range $0<\nu'<0.05$ (see below).

To find M, we use data from Whale et al. on the effect of pressure on specific hydraulic conductivity (K) of the aorta wall in a flat geometry with the endothelium removed. They found that in a range from 0 to 100 mmHg, the mean value of K, defined as $\mu Q h_0/(A\Delta P)$, decreased from approximately 3.5×10^{-14} cm^2 to 1.0×10^{-14} cm^2. In the appendix, we derive the flow-induced deformation and pressure drop associated with flow through an anisotropic, biphasic material mounted in a flat geometry and constrained at the downstream end. Using Eq. (A-6), and the parameter values given above, we find that a value of M of approximately 6 gives model predictions that are in good agreement with this experimental data. Lai and Mow [18] found $M=4.3$ for cartilage.

Whale et al. [14] chose their best-fit value of ν' based on the observation that, in a cylindrical geometry, the measured specific hydraulic conductivity did not depend on perfusion pressure in the range 20–85 mmHg (again, with the endothelium removed). They concluded that the volume of the aortic wall must be relatively constant for this range of pressures. They picked the value of ν' that kept aortic wall volume constant over this pressure range.

We followed a similar procedure and found (see Fig. 1) that a value of ν' of approximately 0.038 gave a nearly constant value of the aortic wall volume over the entire pressure range investigated (note that $M\Psi<<2$ for this best-fit value of ν', justifying our linearization in Eq. (11)). There was significantly less volume variation than for the best-fit parameter found by Whale et al. [14] with their single-phase model. Figure 2 shows that the parameter values chosen to fit the data of Whale et al. with our biphasic model also give excellent agreement with the data on vessel radius, as good as previously found using the single-phase model.

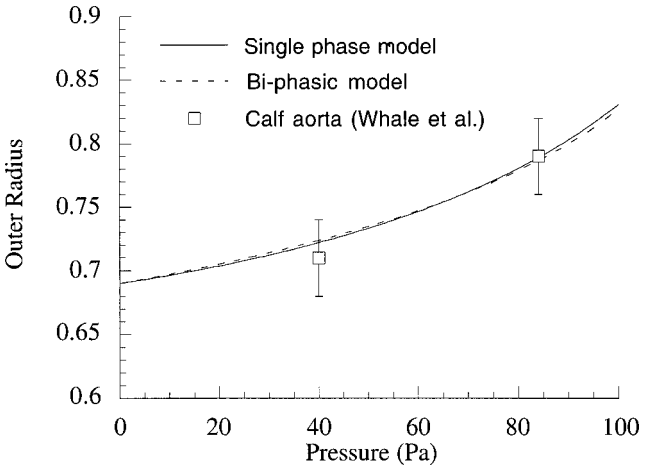

Fig. 2 Biphasic and single-phase [12] model predictions of aortic radius as a function of perfusion pressure for parameter values of $E=460$ kPa, $E'=20$ kPa, $\nu=0.3$, $M=6.0$ and $\nu'=0.038$ (biphasic) or $\nu'=0.0$ (single-phase)

We can use these parameters ($E=460$ kPa, $E'=20$ kPa, $\nu=0.3$, $\nu'=0.038$, $M=6$) and Eqs. (3), (6), (7), and (19) to examine differences in predictions for the stress and strain fields between the single-phase model [12] and the biphasic model. Figures 3 and 4 show the radial and tangential stress and strain fields comparing the single-phase to the biphasic model. While the stress distributions are similar, the strain field is much more uniform in the biphasic model than in the single-phase model, especially the radial strain. This uniformity will be useful when we extend our model below to allow the moduli to be functions of the perfusion pressures.

Application of the Model to the Data of Baldwin et al.

Baldwin et al. [6,19] conducted experiments on rabbit aortas in situ, measuring a variety of parameters as a function of perfusion pressure including aortic diameter, wall thickness, and hydraulic conductivity. The perfusion pressure ranged from 20 to 200

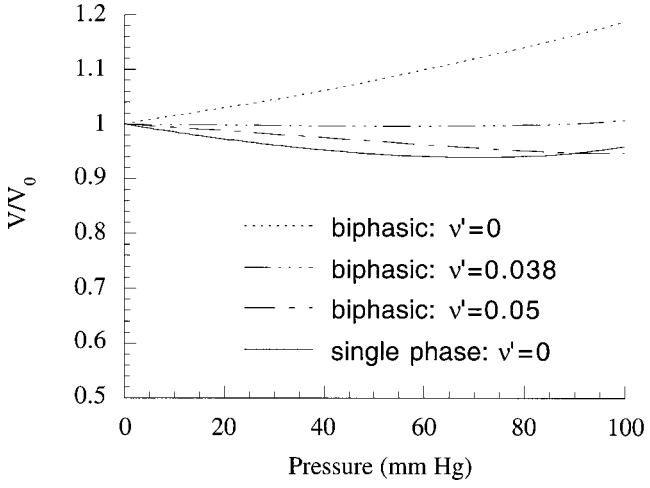

Fig. 1 Biphasic and single-phase [12] model predictions of aortic wall volume (normalized to unpressurized volume) as a function of perfusion pressure in a cylindrical geometry for parameter values of $E=460$ kPa, $E'=20$ kPa, $\nu=0.3$, $M=6.0$, and $0<\nu'<0.05$

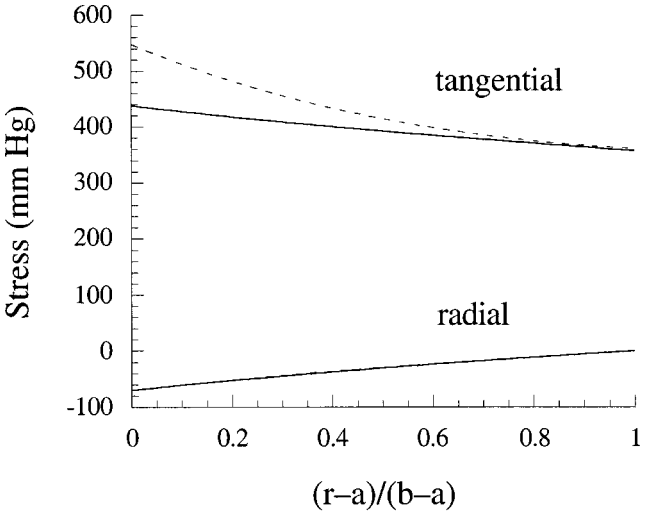

Fig. 3 Comparison of biphasic (solid line) to single-phase model (dashed line) [12] for the tangential (σ_t) and radial (σ_r) stress distribution in the aortic wall at a perfusion pressure of 70 mmHg for parameter values of $E=460$ kPa, $E'=20$ kPa, $\nu=0.3$, $\nu'=0.038$ and $M=6.0$.

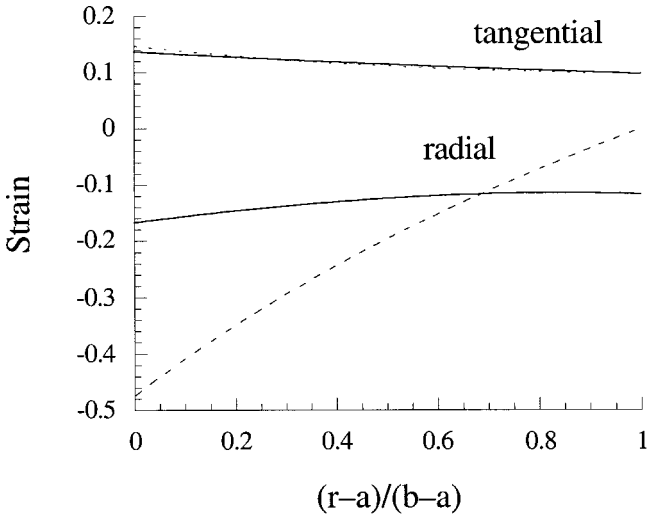

Fig. 4 Comparison of biphasic (solid line) to single-phase model (dashed line) [12] for the tangential (ϵ_t) and radial strain (ϵ_r) distribution in the aortic wall at a perfusion pressure of 70 mmHg for parameter values of $E=460$ kPa, $E'=20$ kPa, $\nu=0.3$, $\nu'=0.038$ and $M=6.0$

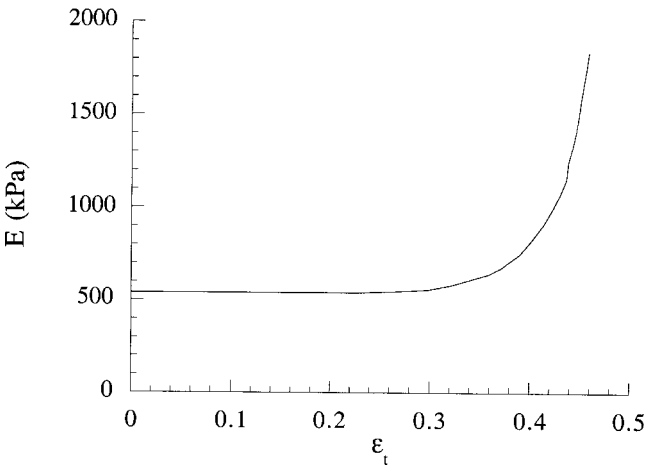

Fig. 6 Modulus in the plane of symmetry (E) of the rabbit aorta as a function of tangential strain as determined by the biphasic model in combination with the data from Baldwin et al. [6]

mmHg, much greater than the range investigated by Whale et al. [14]. Their experiments were done both with the endothelium intact and endothelium removed.

While our model is strictly valid only for the case with the endothelium removed, we can still use our model to investigate the dependence of the vessel radius on perfusion pressure for vessels with thin walls such as those investigated by Baldwin et al. ($\delta/a<0.05$). The model gives good predictions for vessel radius because in the thin wall limit, the stresses acting on the vessel depend only on the total pressure drop and not its distribution as can be seen in Eqs. (24) and (25), which show that the vessel inner and outer radius depend only on ΔP and not on M. Thus, we will use radius data from Baldwin et al. taken with the endothelium intact. However, our model predictions for vessel hydraulic conductivity will only be valid for data taken with the endothelium removed.

We have thus far assumed the modulus of the aortic wall to be a constant. However, it is known that the modulus increases with pressure especially for pressures greater than 100 mmHg [20].

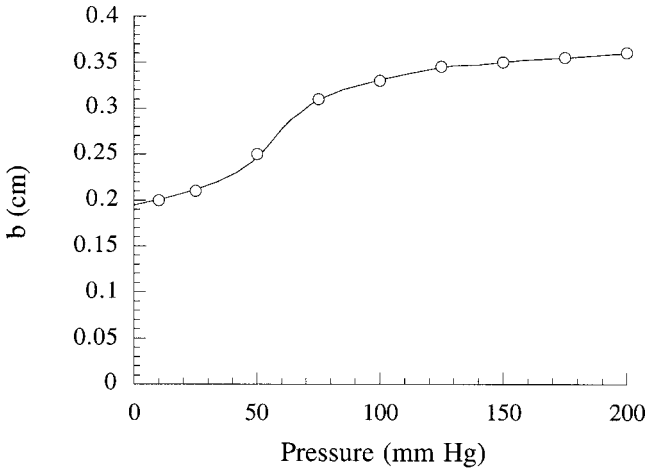

Fig. 5 Data (symbols) from rabbit aorta Baldwin et al. [6] for vessel radius as a function of perfusion pressure. The solid line is from the nonlinear biphasic model as described in the text

Thus, while the constant modulus assumption worked reasonably well for matching the data of Whale et al. [14], it is not expected to match the data of Baldwin et al. [6]. We can demonstrate this using the data from Baldwin et al. [6] at low perfusion pressure (Fig. 3 of that paper).

They found that, for the typical data presented, the outer radius of the vessel increased from 2 to 2.2 mm as the perfusion pressure was increased from 10 to 25 mmHg. Using Eq. (24), we can then estimate the parameter β_{22} as approximately $1.5\times10^{-7}\,\mathrm{Pa}^{-1}$. Equations (24) and (25) can be combined to find a maximum sustainable pressure (the maximum pressure for which these equations have a solution). This criterion is found to be:

$$\Delta P_{\max}\approx\frac{0.17}{\beta_{22}}\left(\frac{\delta_0}{b_0}\right) \tag{27}$$

which, for a vessel having a wall thickness of approximately 150 μm and radius of 2 mm, yields a maximum supportable pressure of roughly 60 mmHg. Since perfusions were conducted up to 200 mmHg, the modulus of the wall must stiffen significantly with increasing pressure.

To model these data, we use the biphasic model as previously described but allow the two moduli to be functions of the perfusion pressure. This approximation is reasonable since the strain level throughout the aortic wall is reasonable uniform for the biphasic model (see Fig. 4). We use the same values for the dimensionless parameters used to model the data of Whale et al. [14]: $\nu=0.3$, $\nu'=0.038$, $M=6$. The modulus in the plane of symmetry, E, is determined by matching the detailed data on vessel radius as a function of pressure (see Fig. 5). We allow the ratio of E'/E to remain fixed, so that E' increases with pressure at the same rate as does E. The unpressurized vessel radius is taken as 0.195 cm (see Fig. 5), and the unpressurized wall thickness as 150 μm (estimate based on data in Fig. 8).

This still leaves unspecified the value of the modulus E' at $P=0$. To determine this, we take advantage of our finding that the volume of the aorta is nearly independent of inflation pressure. For a thin wall, this condition can be approximated as $b\Delta\delta\approx-\delta\Delta b$. Then, using Eqs. (24) and (25), we find:

$$\frac{E'}{E}\approx\frac{\nu'}{1-\nu} \tag{28}$$

Figure 5 shows the data from Baldwin et al. [6] used to determine E. Figure 6 shows the values of E as a function of the

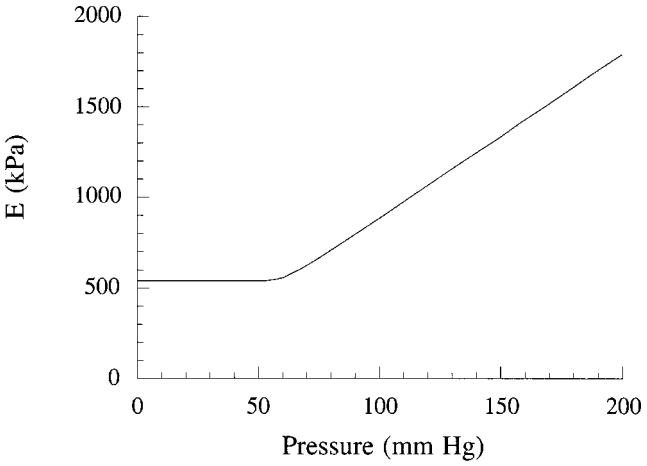

Fig. 7 Modulus in the plane of symmetry (*E*) of the rabbit aorta as a function of perfusion pressure as determined by the biphasic model in combination with the data from Baldwin et al. [6]

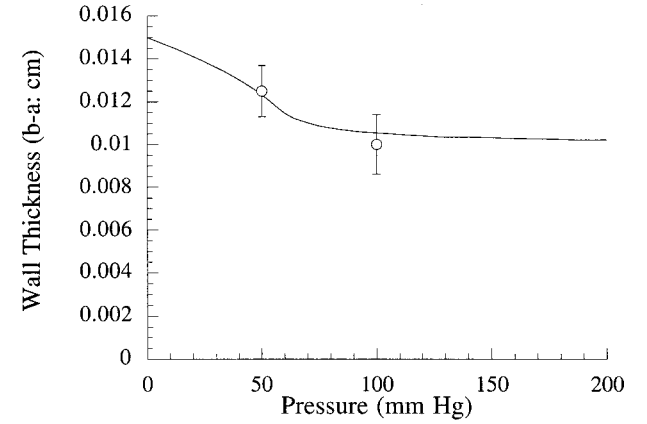

Fig. 8 Thickness of the rabbit aortic wall as predicted by the nonlinear, biphasic model (solid line) for the parameters given in the text. Data shown are from Baldwin et al. [6]

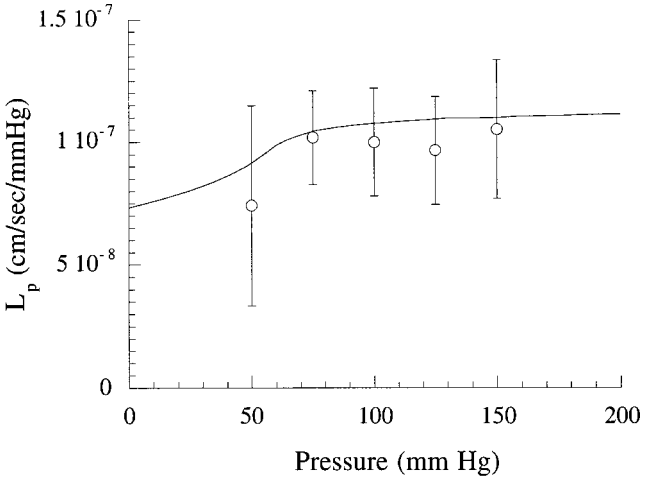

Fig. 9 Hydraulic conductivity of the rabbit aortic wall as predicted by the nonlinear, biphasic model (solid line) for the parameters given in the text. Data shown are from Baldwin et al. [19]

tangential strain. The value of the moduli at zero pressure, $E = 540$ kPa and $E' = 29.3$ kPa, are very similar to the parameters determined in the previous section for bovine aorta. Interestingly, the modulus increases linearly with perfusion pressure for pressures above 60 mmHg (Fig. 7), but is nearly constant at lower pressure, in very good agreement with findings of McDonald [20] in the dog aorta. This supports the use of a constant modulus for the Whale et al. [14] data as that study only considered pressures less than 85 mmHg.

Figures 8 and 9 show that the model gives good predictions for the other parameters measured by Baldwin et al. [6,19]. Figure 8 shows the wall thickness. Not only does the model agree well with the data reported, but it also agrees with the statement in the text of Baldwin et al. [6] that ''no further thinning [of the aortic wall] was noted at 150 mmHg.'' Figure 9 shows the model predictions and data taken for $L_p = (Q/2\pi Lb)/\Delta P$, the hydraulic conductivity of the aortic wall (a value of K_0 of 0.6×10^{-14} cm^2 was chosen). Again, the agreement is good.

Conclusions and Discussion

It is now generally recognized that the aortic wall is a nonlinear [20], biphasic [13,5,8] and anisotropic [10–12] material. As such, these characteristics must be included in any model describing the elastic and transport properties of the aortic wall. We have been able to show that a biphasic, anisotropic model of the aortic wall captures much of its behavior that is seen experimentally.

The model developed in this manuscript yields the same form as that of Klanchar and Tarbell [5] in the limit of an isotropic tissue. However, when Klanchar and Tarbell applied their model to consider the hydraulic conductivity of the aortic wall, measured in a cylindrical vessel, they improperly concluded that the coefficient *M*, which characterizes how the specific hydraulic conductivity of a tissue depends on its bulk dilation, was negative. This error, which has been propagated into several further works [7,21], arose from their attempt to account for the decreased specific hydraulic conductivity of the aortic wall with increasing perfusion pressure that has been reported [22,19].

It now appears that the decreased hydraulic conductivity of the aortic wall observed in these studies was due to the presence of the endothelium [8] and a theoretical explanation of this phenomenon in terms of a deformable intima has been offered [23]. Our model shows that, for an isotropic aortic wall, an increased intraluminal pressure will always lead to a positive bulk dilation of the vessel wall and thus the specific hydraulic conductivity of such a vessel would be expected to increase with an increased pressure. This is not necessarily the case for an anisotropic vessel wall, and one of us has previously speculated [12] that an important function of an anisotropic aortic wall is to maintain constant wall volume with increased intraluminal pressure, as seen in Fig. 1. A relatively constant wall volume would inhibit alterations in the concentrations of extracellular macromolecules that might otherwise change with differing physiological conditions. In fact, our biphasic model shows this constant wall volume condition can be better maintained with a biphasic tissue than with a single-phase tissue.

It is interesting that the tangential and radial moduli predicted for the bovine (460 kPa and 20 kPa, respectively) and the rabbit (540 kPa and 30 kPa) are similar to one another, at least below 100 mmHg. While we did not explicitly include the nonlinear characteristics of the aorta in our model development, use of the model showed that nonlinearity must be considered for perfusion pressures greater than approximately 60 mmHg; McDonald indicates that in the dog, the aortic wall remains linear until approximately 100 mmHg [20]. Our quasi-empirical determination of the modulus necessary to fit the data of Baldwin et al. (Fig. 6) did not show the expected exponential stiffening with increasing strain beginning at $\varepsilon = 0$. Instead, there was a rapid stiffening that began at approximately 30 percent tangential strain. We would suggest that this behavior is consistent with collagen and elastin in the

aortic wall acting in parallel, with the relatively constant modulus elastin acting at low strain and then the collagen beginning to dominate at the higher strain levels.

A final point of interest in this study involves the coefficient M that characterizes the relationship between the specific hydraulic conductivity of a tissue and its volume dilation. Lai and Mow [18] reported a value for $M=4.3$ for cartilage, while in this study, we found the value that best fit our data for compression of aortic wall was $M=6$. Both of these values are much higher than would be expected for the deformation of a fiber matrix model. For small deformations, such as are characterized by equation (11), fiber matrix theory would predict a value of M of approximately 1.17 [24]. This suggests that flow through connective tissues is much more dependent on deformation than fiber matrix theory predicts, and this may imply that preferential flow channels through the tissue exist that are progressively closed as the tissue is deformed. Alternatively, there may be localized regions of high compression that limit fluid flow.

Acknowledgments

JMT was partially supported by NIH Grant No. HL57093 and NASA Grant No. MAG3-1871.

Appendix

We here consider the one-dimensional flow of fluid through a anisotropic, biphasic material that is mounted flat against a porous support and confined in the directions perpendicular to the flow direction $(0<x<h)$.

For this case of confined compression, $\varepsilon_y=\varepsilon_z=0$, and Eq. (4) becomes:

$$S_x=\frac{E'(1-\nu)\varepsilon_x}{1-\nu-2\nu'^2\dfrac{E}{E'}}=E_{confined}\varepsilon_x \tag{A-1}$$

The differential force balance in this geometry yields $d\sigma_x/dx=0$, or $dS_x/dx=dP/dx$. Introducing Eq. (A-1) into this relationship along with the strain definition that $\varepsilon_x=du/dx$ yields:

$$\frac{dP}{dx}=-E_{confined}\frac{d^2u}{dx^2} \tag{A-2}$$

The pressure gradient in this case is found as:

$$\frac{dP}{dx}=\frac{\mu Q}{kA} \tag{A-3}$$

where A is the cross-sectional area facing the flow. We again assume that $K=K_0\exp(M\Psi)$, however, the small strain assumption used to derive Eq. (11) is not applied here since significant volumetric compression is anticipated in this geometry. Using Eqs. (A-2), (A-3), and the relationship between K and Ψ, we find that:

$$\frac{\mu Q}{K_0A}e^{-M(du/dx)}=-E_{confined}\frac{d^2u}{dx^2} \tag{A-4}$$

This differential equation can be solved subject to the boundary conditions that $u(x=0)=0$ and $\epsilon_x(x=h)=0$ to find that:

$$u(h)=h-h_0=-\frac{h}{M}-\frac{K_0E_{confined}}{\mu(Q/A)M^2}\left[\left(1-\frac{\mu(Q/A)hM}{K_0E_{confined}}\right)\times\ln\left(1-\frac{\mu(Q/A)hM}{K_0E_{confined}}\right)\right] \tag{A-5}$$

where h_0 is the undeformed thickness of the medium.

Equation (A-3) can be solved for ΔP by using the solution to Eq. (A-4) in combination with the relationship between K and Ψ to find that:

$$\Delta P=-\frac{E_{confined}}{M}\ln\left[1-\frac{\mu(Q/A)hM}{K_0E_{confined}}\right] \tag{A-6}$$

References

[1] Vargas, C. B., Vargas, F. F., Pribyle, J. G., and Blackshear, B. L., 1979, ''Hydraulic Conductivity of the Endothelial and Outer Layers of Rabbit Aorta,'' Am. J. Physiol., **236**, pp. H53–H60.

[2] Fry, D. L., 1983, ''Effect of Pressure and Stirring on the in Vitro Aortic Transmural ^{125}I-Albumin Transport,'' Am. J. Physiol., **245**, pp. H977–H991.

[3] Parker, K. H., and Winlove, C. P., 1984, ''The Macromolecular Basis of the Hydraulic Conductivity of the Arterial Wall,'' Biorheology, **21**, pp. 181–196.

[4] Tedgui, A., and Lever, M., 1985, ''The Interaction of Convection and Diffusion in the Transport of ^{131}I-Albumin Within the Media of the Rabbit Thoracic Aorta,'' Circ. Res., **57**, pp. 856–863.

[5] Klanchar, M., and Tarbell, J., 1987, ''Modeling Water Flow Through Arterial Tissue,'' Bull. Math. Biol., **49**, pp. 651–669.

[6] Baldwin, A., Wilson, L., and Simon, B., 1992, ''Effect of Pressure on Aortic Hydraulic Conductivity,'' Arterioscler. Thromb., **12**, pp. 163–171.

[7] Kim, W.-K., and Tarbell, J., 1994, ''Macromolecular Transport Through the Deformable Porous Media of an Artery Wall,'' ASME J. Biomech. Eng., **116**, pp. 156–163.

[8] Simon, B., Kaufmann, M., McAfee, M., Baldwin, A., and Wilson, L., 1998, ''Identification and Determination of Material Properties for Porohyperelastic Analysis of Large Arteries,'' ASME J. Biomech. Eng., **120**, pp. 188–194.

[9] Bergel, D. H., 1961, ''The Static Elastic Properties of the Arterial Wall,'' J. Physiol. (Lond), **156**, pp. 445–457.

[10] Fenn, W. O., 1957, ''Changes in Length of Blood Vessels on Inflation,'' in: *Tissue Elasticity*, J. W. Remington, ed., American Physiological Society, Washington, DC, pp. 154–167.

[11] Tickner, E. G., and Sacks, A. H., 1967, ''A Theory for the Static Elastic Behavior of Blood Vessels,'' Biorheology, **4**, pp. 151–168.

[12] Whale, M. D., Grodzinsky, A. J., and Johnson, M., 1996, ''The Effect of Aging and Pressure on the Specific Hydraulic Conductivity of the Aortic Wall,'' Biorheology, **33**, pp. 17–44.

[13] Kenyon, D. E., 1979, ''A Mathematical Model of Water Flux Through Aortic Tissue,'' Bull. Math. Biol., **41**, pp. 79–90.

[14] Whale, M. D., Grodzinsky, A. J., and Johnson, M., 1996, ''The Effects of Age and Pressure on the Specific Hydraulic Conductivity of the Aortic Wall,'' Biorheology, **33**, pp. 17–44.

[15] Loree, H. M., Kamm, R. D., Stringfellow, R. G., and Lee, R. T., 1992, ''Effects of Fibrous Cap Thickness on Peak Circumferential Stress in Model Atherosclerotic Vessels,'' Circ. Res., **71**, pp. 850–858.

[16] Lehknitskii, S. G., 1963, *Theory of Elasticity of an Anisotropic Body*, Holden-Day, San Francisco, CA.

[17] Levick, J. R., 1987, ''Flow Through Interstitum and Other Fibrous Matrices,'' Q. J. Exp. Physiol. (1981), **72**, pp. 409–437.

[18] Lai,, W. and Mow, V., 1980, ''Drag Induced Compression of Articular Cartilage During a Permeation Experiment,'' Biorheology, **17**, pp. 111–123.

[19] Baldwin, A., and Wilson, L., 1993, ''Endothelium Increases Medial Hydraulic Conductance of Aorta, Possibly by Release of EDRF,'' Am. J. Physiol., **264**, pp. H26–H32.

[20] McDonald, D. A., 1974, ''The Elastic Properties of the Arterial Wall,'' in: *Blood Flow in Arteries*, Williams and Wilkins Co., Baltimore, MD, pp. 238–282.

[21] Dhar, P., Jayaraman, G., Karmakar, N., and Manchanda, S., 1996, ''Effect of Pressure on Transmural Fluid Flow in Different De-Endothelialised Arteries,'' Med. Biol. Eng. Comput., **34**, pp. 155–159.

[22] Tedgui, A., and Lever, M. J., 1984, ''Filtration Through Damaged and Undamaged Rabbit Thoracic Aorta,'' Am. J. Physiol., **247**, pp. H784–H791.

[23] Huang, Y., Rumschitzki, D., Chien, S., and Weinbaum, S., 1997, ''A Fiber Matrix Model for the Filtration Through Fenestral Pores in a Compressible Arterial Intima,'' Am. J. Physiol., **272**, pp. H2023–H2039.

[24] Ethier, C. R., 1986, ''The Hydrodynamic Resistance of Hyaluronic Acid: Estimates From Sedimentation Studies,'' Biorheology, **23**, pp. 99–113.